

# Search of wormholes in different dimensional non-commutative inspired space-time with Lorentzian distribution

Piyali Bhar<sup>1,\*</sup> and Farook Rahaman<sup>1,†</sup>

<sup>1</sup> *Department of Mathematics, Jadavpur University, Kolkata 700 032, West Bengal, India*

In this paper we are interested to search whether the wormhole solutions exists in different dimensional noncommutative inspired spacetime. It is well known that the noncommutativity of the space is an outcome of string theory and it replaced the usual point like object by a smeared object. Here we have chosen Lorentzian distribution as the density function in the noncommutative inspired spacetime. We have observed that the wormhole solutions exist only in four and five dimension, however, higher than five dimension no wormhole exists.

PACS numbers:

## I. INTRODUCTION

Wormhole is a hypothetical topological feature of the spacetime which connects two distinct spacetimes. Morris and Thorne [1] have shown that wormhole geometry could be found by solving Einstein field equation by violating the null energy condition (NEC) which is threaded as exotic matter. There are a large number of works [2, 3, 4] based on the concept of Morris and Throne.

Recent years researchers have shown considerable interest on the study of noncommutative spaces. One of the most interesting outcomes of the string theory is that the target spacetimes coordinates becomes noncommuting operators on D-brane [5]. Now the noncommutativity of a spacetime can be encoded in the commutator  $[x^\mu, x^\nu] = i\theta^{\mu\nu}$ , where  $\theta^{\mu\nu}$  is an anti-symmetric matrix and is of dimension  $(length)^2$  which determines the fundamental cell discretization of spacetime. It is similar to the way that the plank constant  $\hbar$  discretizes phase space [6]. In noncommutative space the usual definition of mass density in the form of Dirac delta function does not hold. So in noncommutative spaces the usual form of the energy density of the static spherically symmetry smeared and particlelike gravitational source in the form of Lorentzian distribution is [7]

$$\rho = \frac{M\sqrt{\phi}}{\pi^2(r^2 + \phi)^{\frac{n+2}{2}}}$$

Here, the mass  $M$  could be the mass of diffused centralized object such as a wormhole and  $\phi$  is noncommutative parameter.

There are many works inspired by noncommutative geometry in literature. Nazari *et al.* [7] used Lorentzian distribution to analyze 'Parikh-Wilczek Tunneling from Noncommutative Higher Dimensional Black Holes'. [8]

Rahaman *et al* have shown that a noncommutative geometrical background is sufficient for the existence of a stable circular orbit and one does not need to consider dark matter for galactic rotation curve. Kuhfittig [9] found that a special class of thin shell wormholes could be possible that are unstable in classical general relativity but are stable in a small region in noncommutative spacetime. By taking Gaussian distribution as the density function Rahaman *et al* [10] have shown that wormhole solutions exists in usually four as well as in five dimensions only. Banerjee *et al* [11] has made a detailed investigation on thermodynamical study e.g. Hawking temperature, entropy and the area law for Schwarzschild black hole in the noncommutative spacetime. Noncommutative Wormholes in  $f(R)$  Gravity with Lorentzian Distribution has been analyzed in [12]. BTZ black hole inspired by noncommutative geometry has been discussed in [13].

Recently, the extension of general relativity in higher dimension has become a topic of great interest. The discussion in higher dimensions is essential due to the fact that many theories indicate that extra dimensions exist in our Universe. Higher dimensional gravastar has been discussed by Rahaman *et al* [14]. Rahaman *et al* [15] have investigated whether the usual solar system tests are compatible with higher dimensions. Another studies in higher dimension are the motion of test particles in the gravitational field of higher dimensional black hole [16].

Inspired by all of these previous work, we are going to analyze whether wormhole solutions exists in four and higher dimensional spacetime in noncommutative inspired geometry where energy distribution function is taken as Lorentzian distribution.

The plan of our paper as follows: In section II we have formulated basic Einstein field equations. In section III, we have solved those fields equations in different dimensions and in section IV the linearized stability analysis for four dimensional spacetime has been worked out. Some discussions and concluding remarks have

\*Electronic address: piyalibhar90@gmail.com

†Electronic address: rahaman@iucaa.ernet.in

been done in the final section.

## II. EINSTEIN FIELD EQUATION IN HIGHER DIMENSION

To describe the static spherically symmetry spacetime (in geometrical unit  $G = 1 = c$  here and onwards) in higher dimension, we consider the line element is in the standard form as

$$ds^2 = -e^{\nu(r)} dt^2 + e^{\lambda(r)} dr^2 + r^2 d\Omega_n^2 \quad (1)$$

where

$$d\Omega_n^2 = d\theta_1^2 + \sin^2 \theta_1 d\theta_2^2 + \sin^2 \theta_1 \sin^2 \theta_2 d\theta_3^2 + \dots + \prod_{i=1}^{n-1} \sin^2 \theta_i d\theta_n^2 \quad (2)$$

The most general form of the energy momentum tensor for the anisotropic matter distribution can be taken as [2]

$$T_\nu^\mu = (\rho + p_r) u^\mu u_\nu - p_r g_\nu^\mu + (p_t - p_r) \eta^\mu \eta_\nu \quad (3)$$

with  $u^\mu u_\mu = -\eta^\mu \eta_\mu = 1$ .

Here  $\rho$  is the energy density,  $p_r$  and  $p_t$  are respectively the radial and transverse pressures of the fluid.

In higher dimensions, Einstein field Equations can be written as [10]

$$e^{-\lambda} \left( \frac{n\lambda'}{2r} - \frac{n(n-1)}{2r^2} \right) + \frac{n(n-1)}{2r^2} = 8\pi\rho \quad (4)$$

$$e^{-\lambda} \left( \frac{n(n-1)}{2r^2} + \frac{n\nu'}{2r} \right) - \frac{n(n-1)}{2r^2} = 8\pi p_r \quad (5)$$

$$\begin{aligned} \frac{1}{2} e^{-\lambda} \left[ \frac{1}{2} (\nu')^2 + \nu'' - \frac{1}{2} \lambda' \nu' + \frac{(n-1)}{r} (\nu' - \lambda') \right] \\ + \frac{(n-1)(n-2)}{2r^2} (e^{-\lambda} - 1) = 8\pi p_t \end{aligned} \quad (6)$$

Here 'prime' denotes the differentiation with respect to the radial parameter  $r$ .

In higher dimension, the density function of a static and spherically symmetric Lorentzian distribution of smeared matter as follows [7]

$$\rho = \frac{M\sqrt{\phi}}{\pi^2(r^2 + \phi)^{\frac{n+2}{2}}} \quad (7)$$

where  $M$  is the smeared mass distribution.

## III. MODEL OF THE WORMHOLE

Let us assume the constant redshift function for our model, so called tidal force solution. So we have,

$$\nu = \nu_0 \quad (8)$$

where  $\nu_0$  is a constant.

Using equation (8) Einstein field equations becomes,

$$\frac{nb'}{2r^2} + \frac{n(n-2)b}{2r^3} = \frac{8\pi M\sqrt{\phi}}{\pi^2(r^2 + \phi)^{\frac{n+2}{2}}} \quad (9)$$

$$8\pi p_r = -\frac{n(n-1)}{2r^3} b \quad (10)$$

$$8\pi p_t = \frac{(3-n)(n-1)}{2r^3} b - \frac{(n-1)b'}{2r^2} \quad (11)$$

where  $b(r) = r(1 - e^{-\lambda})$  and  $\nu(r)$  termed as the shape function and the redshift function respectively of the wormhole.

From equation (9) we get,

$$b(r) = \frac{16M\sqrt{\phi}}{n\pi} \frac{1}{r^{n-2}} \int \frac{r^n}{(r^2 + \phi)^{\frac{n+2}{2}}} dr + \frac{C}{r^{n-2}} \quad (12)$$

Now, the following criterions need to be imposed for the existence of a wormhole solution.

1. The redshift function  $\nu(r)$  must be finite everywhere ( traversability criteria )
2.  $\frac{b(r)}{r} \rightarrow 0$  as  $n \rightarrow \infty$  ( asymptotically flat spacetime )
3. At the throat ( $r_0$ ) of the wormhole  $b(r_0) = r_0$  and  $b'(r_0) < 1$  ( flaring out condition )
4.  $b(r) < r$  for  $r > r_0$  (regularity of metric coefficient)

### A. Four dimensional Spacetime (n=2)

In four dimensional spacetime, the shape function of the wormhole is given by,

$$b(r) = \frac{4M\sqrt{\phi}}{\pi} \left\{ \frac{1}{\sqrt{\phi}} \tan^{-1} \left( \frac{r}{\sqrt{\phi}} \right) - \frac{r}{r^2 + \phi} \right\} + C \quad (13)$$

where, C is an integration constant.

The radial and transverse pressure can be obtained as

$$8\pi p_r = -\frac{1}{r^3} \left[ \frac{4M\sqrt{\phi}}{\pi} \left\{ \frac{1}{\sqrt{\phi}} \tan^{-1} \left( \frac{r}{\sqrt{\phi}} \right) - \frac{r}{r^2 + \phi} \right\} + C \right] \quad (14)$$

$$8\pi p_t = \frac{1}{2r^3} \left[ \frac{4M\sqrt{\phi}}{\pi} \left\{ \frac{1}{\sqrt{\phi}} \tan^{-1}\left(\frac{r}{\sqrt{\phi}}\right) - \frac{r}{r^2 + \phi} \right\} + C \right] - \frac{4M\sqrt{\phi}}{\pi} \frac{1}{(r^2 + \phi)^2} \quad (15)$$

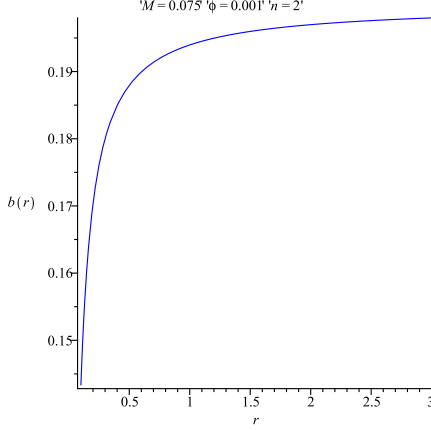


FIG. 1: Diagram of the shape function of the wormhole in four dimension is shown against  $r$ .

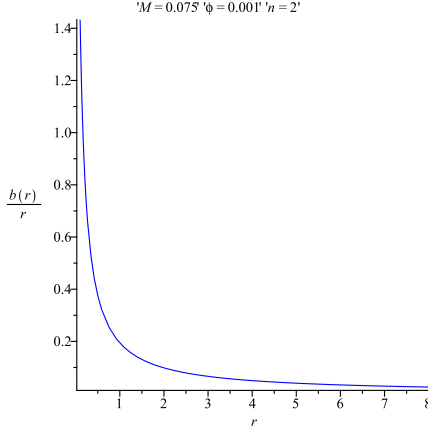


FIG. 2: Asymptotically flatness condition in four dimensional spacetime is shown against  $r$ .

Next, we are going to verify whether the shape function  $b(r)$  (see FIG. 1) satisfies all the physical requirements to form a wormhole structure (which has been given in section III). For this purpose we assign some arbitrary values to the parameters (mentioned in the figures). From FIG. 2, we see that  $\frac{b(r)}{r} \rightarrow 0$  as  $r \rightarrow \infty$  which verifies that the spacetime is asymptotically flat. The throat  $r_0$  of the wormhole occurs where  $b(r_0) = r_0$ , which is the root of the function  $G(r) = b(r) - r$ . We have plotted  $G(r)$  Vs.  $r$  in FIG. 3. The throat of the wormhole occurs where  $G(r)$  cuts the  $r$  axis. From the figure we see

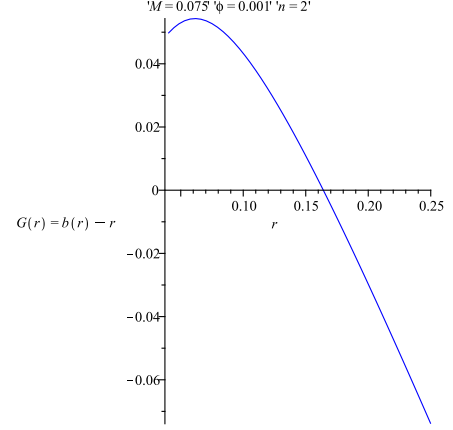


FIG. 3: The throat of the wormhole in 4D occurs where  $G(r)$  cuts the  $r$ -axis.

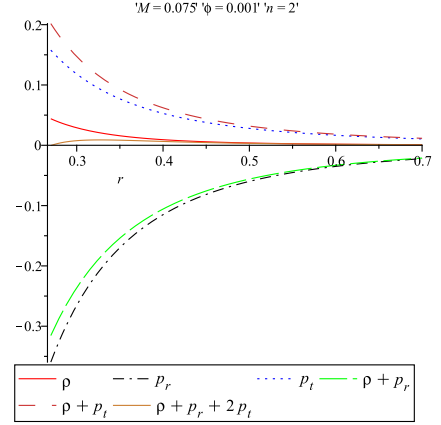


FIG. 4: The energy condition in 4D is shown against  $r$

that  $r = 0.165$ . FIG. 3 also indicates that  $G(r) < 0$  when  $r > r_0$  which implies  $\frac{b(r)}{r} < 1$  when  $r > r_0$ . One can also notice from equation (9) that at the throat of the wormhole ( $r = 0.165$ )  $b'(0.165) = 0.207 < 1$ . Hence Flare-out condition is also satisfied.

According to Morris & Thorne [1] the embedding surface of the wormhole is denoted by the function  $z(r)$  which satisfies the following differential equation

$$\frac{dz}{dr} = \pm \frac{1}{\sqrt{\frac{r}{b(r)} - 1}} \quad (16)$$

The above equation  $\frac{dz}{dr}$  diverges at the throat of the wormhole which concludes that the embedding surface is vertical at the throat.

Equation (16) gives,

$$z = \pm \int_{r_0}^r \frac{dr}{\sqrt{\frac{r}{b(r)} - 1}} \quad (17)$$

TABLE I: Values of  $z(r)$  for different  $r$ .  $r_0^+ = 0.17$ ,  $\phi = 0.001$ ,  $M = 0.075$

$r$	$z(r)$
2	0.9462904189
4	1.476685471
6	1.881582603
8	2.222220748
10	2.521990341
12	2.792809650

TABLE II: Values of  $l(r)$  for different  $r$ .  $r_0^+ = 0.17$ ,  $\phi = 0.001$ ,  $M = 0.075$

$r$	$l(r)$
2	2.053236413
4	4.106613071
6	6.137481048
8	8.159285247
10	10.17615752
12	12.18992251
14	14.20154866

The proper radial distance of the wormhole is given by

$$l(r) = \pm \int_{r_0^+}^r \frac{dr}{\sqrt{1 - \frac{b(r)}{r}}} \quad (18)$$

$$\mathcal{P} = \frac{1}{8\pi R} \left[ \frac{1 - \frac{m}{R} + \dot{R} + R\ddot{R}}{\sqrt{1 - \frac{2m}{R} + \dot{R}^2}} - \frac{1 - \frac{b(R)}{R} + \dot{R}^2 + R\ddot{R} - \frac{\dot{R}^2}{2} \frac{b-b'R}{R-b}}{\sqrt{1 - \frac{b(R)}{R} + \dot{R}^2}} \right] \quad (21)$$

The mass of the thin shell ( $m_s$ ) is given by

$$m_s = 4\pi R^2 \sigma \quad (22)$$

Using the expression of  $\sigma$  in equation (20) (considering the static case) one can obtain the mass of the wormhole as

$$m = \frac{b(R)}{2} - \frac{m_s}{2} \left[ \frac{m_s}{R} + 2\sqrt{1 - \frac{b(R)}{R}} \right] \quad (23)$$

This gives the mass of the wormhole in terms of the thin shell mass.

Let us use the conservation identity given by

$$S_{j,i}^i = -[\dot{\sigma} + 2\frac{\dot{R}}{R}(\mathcal{P} + \sigma)]$$

which gives the following expression

$$\sigma' = -\frac{2}{R}(\mathcal{P} + \sigma) + \Xi \quad (24)$$

(here,  $r_0$  is the throat of the wormhole.) The above two integrals mentioned in equation (17) and (18) can not be done analytically. But we can perform it numerically. The numerical values are obtained by fixing a particular value of lower limit and by changing the upper limit, which are given in Table-I and Table-II respectively. The embedding diagram  $z(r)$  and the radial proper distance  $l(r)$  of 4D wormhole have been depicted in fig. 5 and fig. 7 respectively. Fig. 6 represents the full visualization of 4D wormhole obtained by rotating the fig. 5 about 'z-axis'. We can match our interior wormhole spacetime with the Schwarzschild exterior spacetime

$$ds^2 = -\left(1 - \frac{2m}{r}\right) dt^2 + \frac{dr^2}{1 - \frac{2m}{r}} + r^2 d\Omega_2^2 \quad (19)$$

where

$$d\Omega_2^2 = d\theta^2 + \sin^2 \theta d\phi^2$$

Now by using Darmois-Israel[17, 18] junction condition the surface energy density ( $\sigma$ ) and surface pressure ( $\mathcal{P}$ ) at the junction surface  $r = R$  can be obtained as,

$$\sigma = -\frac{1}{4\pi R} \left[ \sqrt{1 - \frac{2m}{R} + \dot{R}^2} - \sqrt{1 - \frac{b(R)}{R} + \dot{R}^2} \right] \quad (20)$$

where  $\Xi$  is given by,

$$\Xi = -\frac{1}{4\pi R} \frac{b - b'R}{2(R - b)} \sqrt{1 - \frac{b(R)}{R} + \dot{R}^2} \quad (25)$$

The above expression  $\Xi$  will be used to discuss the stability analysis of the wormhole.

From equation (22) we get,

$$\left(\frac{m_s}{2a}\right)'' = \Upsilon - 4\pi\sigma'\eta$$

where

$$\eta = \frac{\mathcal{P}'}{\sigma'} \quad \text{and} \quad \Upsilon = \frac{4\pi}{R}(\sigma + \mathcal{P}) + 2\pi R\Xi'$$

Where the parameter  $\sqrt{\eta}$  is generally denotes the velocity of the sound. So one must have  $0 < \eta \leq 1$

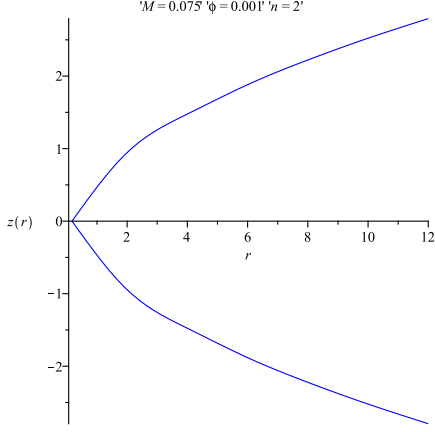


FIG. 5: The embedding diagram of 4D wormhole has been shown against  $r$

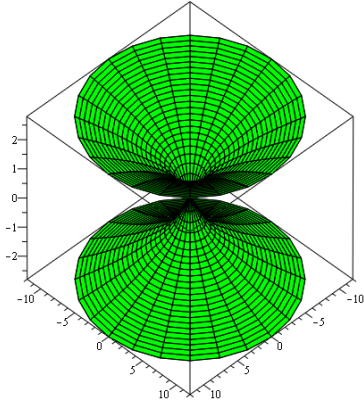


FIG. 6: The full visualization of 4D wormhole surface is obtained by rotating the figure 5 with respect to 'z-axis'

### B. Five dimensional Spacetime (n=3)

In five dimensional spacetime, the shape function of the wormhole is given by,

$$b(r) = \frac{1}{r} \left\{ -\frac{16M\sqrt{\phi}}{9\pi} \frac{3r^2 + 2\phi}{(r^2 + \phi)^{\frac{3}{2}}} + C \right\} \quad (26)$$

The radial and transverse pressures can be obtained as,

$$8\pi p_r = -\frac{3}{r^4} \left\{ -\frac{16M\sqrt{\phi}}{9\pi} \frac{3r^2 + 2\phi}{(r^2 + \phi)^{\frac{3}{2}}} + C \right\} \quad (27)$$

$$8\pi p_t = \frac{1}{r^4} \left\{ -\frac{16M\sqrt{\phi}}{9\pi} \frac{3r^2 + 2\phi}{(r^2 + \phi)^{\frac{3}{2}}} + C \right\} - \frac{16M\sqrt{\phi}}{3\pi} \frac{1}{(r^2 + \phi)^{\frac{5}{2}}} \quad (28)$$

Next our aim is to verify whether  $b(r)$  (see Fig.8) satisfies all the physical requirement to form a shape function.

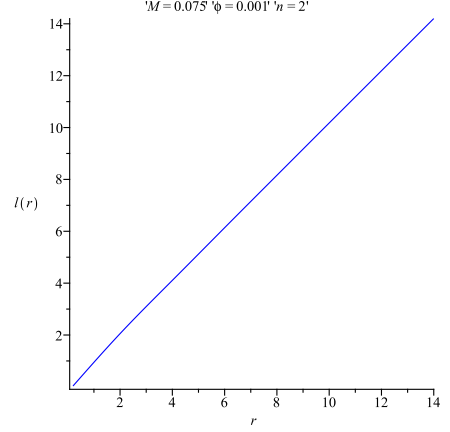


FIG. 7: The radial proper length of the 4D wormhole has been shown against ' $r$ '

From FIG. 9 we see that  $\frac{b(r)}{r} \rightarrow 0$  as  $n \rightarrow \infty$  so space-time is asymptotically flat. The throat of the wormhole is the point where  $G(r) = b(r) - r$  cuts the  $r$  axis. From FIG. 10 we see that  $G(r)$  cuts the ' $r$ ' axis at 0.16, so the throat of the wormhole occurs at  $r = 0.16$  for 5D space-time. Consequently, we see that  $b'(0.16) = 0.89 < 1$ . For  $r > r_0$ , we see that  $b(r) - r < 0$  which implies  $\frac{b(r)}{r} < 1$  for  $r > r_0$ . The slope is still positive up to  $r_1 = 0.22$  but soon it becomes negative ( see fig. 11). So we have a valid wormhole solution from the throat up to a certain radius, say,  $r_1 = .22$ , which is a convenient cut-off for the wormhole. This indicates we get a restricted class of wormhole in five dimensional spacetime. In this case we can match our interior solution to the exterior 5D line element given by

$$ds^2 = - \left( 1 - \frac{2\mu}{r^2} \right) dt^2 + \left( 1 - \frac{2\mu}{r^2} \right)^{-1} dr^2$$

$$+ r^2 (d\theta_1^2 + \sin^2 \theta_1 d\theta_2^2 + \sin^2 \theta_1 \sin^2 \theta_2 d\theta_3^2)$$

where  $\mu$ , the mass of the 5D wormhole, is defined by  $\mu = \frac{4Gm}{3\pi}$ . To obtain the profile of embedding diagram and radial proper distance in  $\theta_3 = 0$  plane of 5D wormhole we have to find out the integral of equation (17) and (18) respectively. But we cannot perform it analytically. So we will take the help of numerical integration. The numerical values are obtained by fixing a particular value of lower limit and by changing the upper limit, which are given in Table-III and Table-IV respectively. The embedding diagram  $z(r)$  and the radial proper distance  $l(r)$  of 4D wormhole have been depicted in fig. 13 and fig. 12 respectively. Fig. 14 represents the full visualization of 5D wormhole obtained by rotating the fig. 13 about 'z-axis'

TABLE III: Values of  $z(r)$  of 5D spacetime for different  $r$ .  
 $r_0^+ = 0.16$ ,  $\phi = 0.001$ ,  $M = 0.075$

$r$	$z(r)$
0.17	0.0221068505
0.175	0.0388300822
0.18	0.0527692279
0.19	0.0758115765
0.20	0.0948891894
0.21	0.1114219209

### C. Six and Seven dimensional Spacetime (n=4) and (n=5)

In six dimensional spacetime, the shape function of the wormhole is given by,

$$b(r) = \frac{1}{r^2} \left[ \frac{M\sqrt{\phi}}{2\pi} \left\{ \frac{3}{\sqrt{\phi}} \tan^{-1} \left( \frac{r}{\sqrt{\phi}} \right) - \frac{5r^3 + 3r\phi}{(r^2 + \phi)^2} \right\} + C \right] \quad (29)$$

The other parameters are given by

$$8\pi p_r = -\frac{6}{r^5} \left[ \frac{M\sqrt{\phi}}{2\pi} \left\{ \frac{3}{\sqrt{\phi}} \tan^{-1} \left( \frac{r}{\sqrt{\phi}} \right) - \frac{5r^3 + 3r\phi}{(r^2 + \phi)^2} \right\} + C \right] \quad (30)$$

$$8\pi p_t = \frac{3}{2r^5} \left[ \frac{M\sqrt{\phi}}{2\pi} \left\{ \frac{3}{\sqrt{\phi}} \tan^{-1} \left( \frac{r}{\sqrt{\phi}} \right) - \frac{5r^3 + 3r\phi}{(r^2 + \phi)^2} \right\} + C \right] - \frac{6M\sqrt{\phi}}{\pi} \frac{1}{(r^2 + \phi)^3} \quad (31)$$

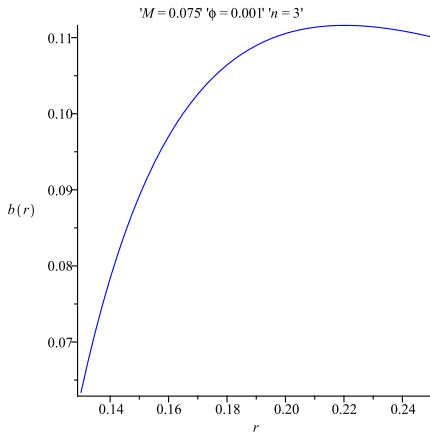


FIG. 8: Diagram of the shape function of the wormhole in five dimension is shown against  $r$

Next we want to verify whether  $b(r)$  obeys the physical conditions (see sec III) to be a shape function of a wormhole. From FIG.(16) we see that  $b(r)$  is a

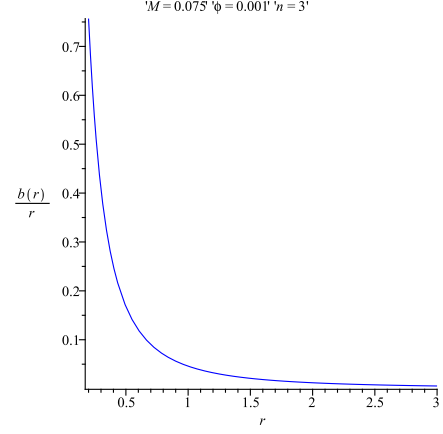


FIG. 9: Diagram of the flatness of the wormhole spacetime in five dimension is shown against  $r$

TABLE IV: Values of  $l(r)$  of 5D spacetime for different  $r$ .  
 $r_0^+ = 0.165$ ,  $\phi = 0.001$ ,  $M = 0.075$

$r$	$l(r)$
0.17	0.2267089806
0.18	0.5493836396
0.19	0.8006389468
0.20	0.1016074351
0.21	0.1209317737

strictly decreasing function of  $r$ , the same situation arises in seven dimensional spacetime ( $n = 5$ ). In seven dimensional spacetime the shape function of the wormhole (see FIG. 17) is given by,

$$b(r) = \frac{1}{r^3} \left[ -\frac{16M\sqrt{\phi}}{75\pi} \frac{15r^4 + 20r^2\phi + 8\phi^2}{(r^2 + \phi)^{\frac{5}{2}}} + C \right] \quad (32)$$

So it is clear that no wormhole solutions exist for  $n > 3$  because for  $n > 3$  the shape function  $b(r)$  (see eq.(12))

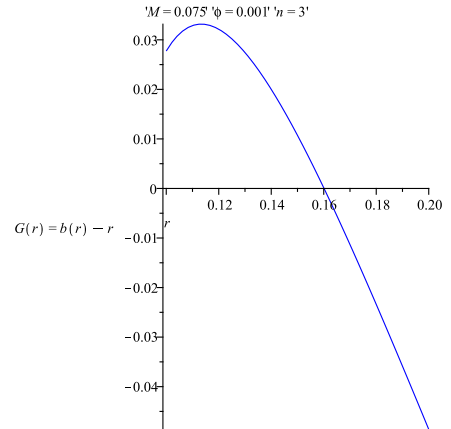


FIG. 10: The throat of the wormhole in 5D case.

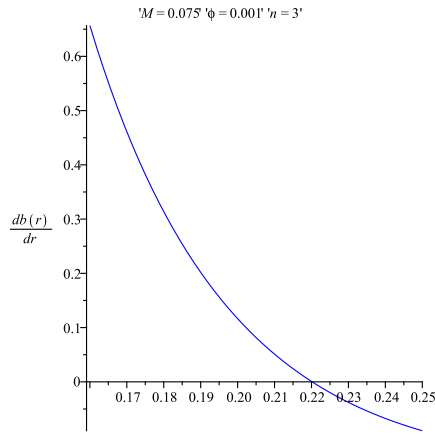


FIG. 11: The slope is still positive up to  $r_1 = 0.22$  but soon becomes negative.

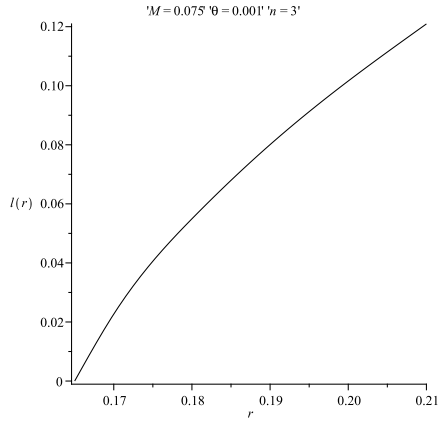


FIG. 12: The radial proper distance of the 5D wormhole in  $\theta_3 = 0$  plane

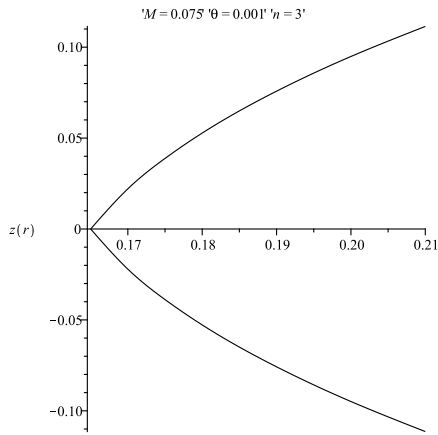


FIG. 13: The embedding diagram of 5D wormhole in  $\theta_3 = 0$  plane

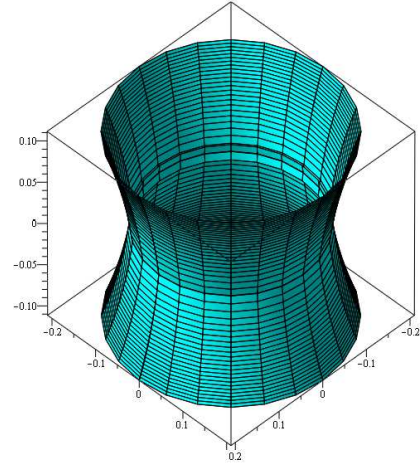


FIG. 14: The full visualization of 5D wormhole in  $\theta_3 = 0$  plane

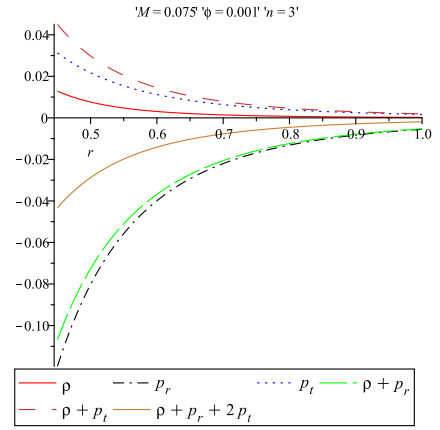


FIG. 15: Diagram of Energy condition for 5D wormhole has been plotted against  $r$

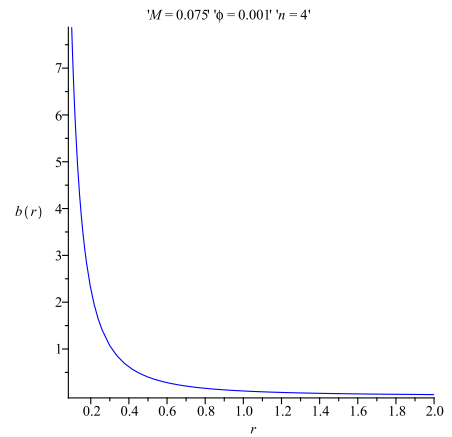


FIG. 16: Diagram of the shape function of the wormhole in six dimension is shown against  $r$

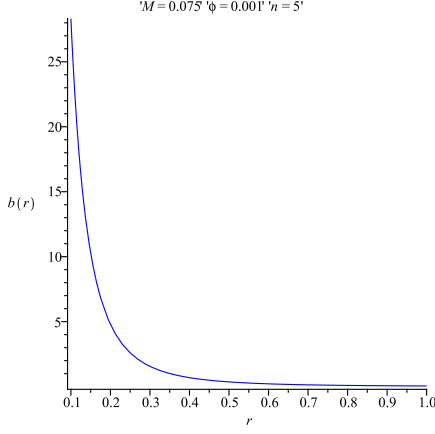


FIG. 17: Diagram of the shape function of the wormhole in seven dimension is shown against  $r$

contains a factor  $\frac{1}{r^{n-2}}$  and if we consider  $n > 3$  the shape function becomes monotonically decreasing for this factor, as a result  $b(r)$  fails to be a shape function.

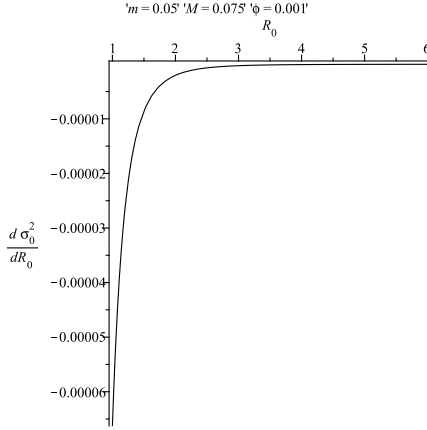


FIG. 18:  $\frac{d\sigma_0^2}{dR_0}$  has been plotted against  $R_0$

#### D. Energy Condition

In this subsection, we are going to verify whether our particular model of wormholes (both 4D and 5D) satisfies all the energy conditions namely null energy condition (NEC), weak energy condition (WEC), strong energy condition (SEC) stated as follows :

$$\rho \geq 0 \quad (33)$$

$$\rho + p_r \geq 0 \quad (34)$$

$$\rho + p_t \geq 0 \quad (35)$$

$$\rho + p_r + 2p_t \geq 0 \quad (36)$$

The profile of energy conditions for four and five dimensional wormhole have been shown in *Fig.4* and *Fig.15* respectively. The figure indicates that  $\rho + p_r < 0$  i.e. the null energy condition (NEC) is violated which is one of the fundamental properties of the wormhole.

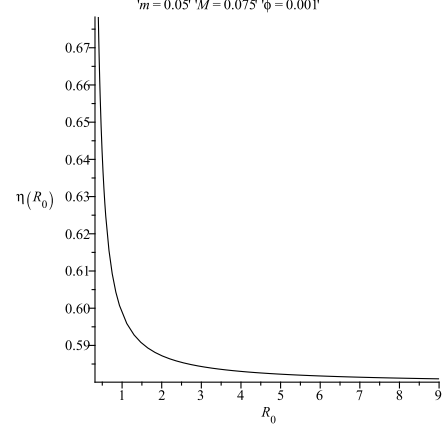


FIG. 19: Plot of  $\eta(R_0)$  vs.  $R_0$

#### IV. LINEARIZED STABILITY ANALYSIS

In this section, we will focus on the stability of the wormhole in four dimensional spacetime ( $n=2$ ).

using the expression of (20) in equation (22) and rearranging we get

$$\dot{R}^2 + V(R) = 0 \quad (37)$$

where  $V(R)$  is given by

$$V(R) = F(R) - \left(\frac{m_s}{2R}\right)^2 - \left(\frac{2m - b(R)}{2m_s(R)}\right)^2$$

$$\text{where } F(R) = 1 - \frac{b+2m}{2R}$$

(for details calculation see the appendix.)

To discuss the linearized stability analysis let us take a linear perturbation around a static radius  $R_0$ . Expanding  $V(R)$  by Taylor series around the radius of the static solution  $R = R_0$ , one can obtain

$$V(R) = V(R_0) + (R - R_0)V'(R_0) + \frac{(R - R_0)^2}{2}V''(R_0) + O[(R - R_0)^3] \quad (38)$$

where 'prime' denotes derivative with respect to 'R'. Since we are linearizing around static radius  $R = R_0$  we



must have  $V(R_0) = 0, V'(R_0) = 0$ . The configuration will be stable if  $V(R)$  has a local minimum at  $R_0$  i.e. if

$$\left(\frac{m_s(R_0)}{2R_0}\right)' = \left(\frac{R_0}{m_s(R_0)}\right) \left[ F'(R_0) - 2 \left(\frac{2m - b(R_0)}{2m_s(R_0)}\right) \left(\frac{2m - b(R_0)}{2m_s(R_0)}\right)' \right] \quad (39)$$

$$V''(R) = F''(R) - 2 \left(\frac{m_s(R)}{2R}\right) \left(\frac{m_s(R)}{2R}\right)'' - 2 \left\{ \left(\frac{m_s(R)}{2R}\right)' \right\}^2 - 2 \left(\frac{2m - b(R)}{2m_s(R)}\right) \left(\frac{2m - b(R)}{2m_s(R)}\right)'' - 2 \left\{ \left(\frac{2m - b(R)}{2m_s(R)}\right)' \right\}^2$$

Now the configuration will be stable if  $V''(R_0) > 0$ . i.e. if

$$\Omega_0 > 2\pi R_0 \sigma_0 \left(\frac{m_s(R)}{2R}\right)'' \Big|_{R=R_0} \quad (40)$$

where  $\Omega_0$  is given by

$$\Omega_0 = \frac{F''(R_0)}{2} - \left\{ \left(\frac{m_s(R_0)}{2R_0}\right)' \right\}^2 - \left(\frac{2m - b(R_0)}{2m_s(R_0)}\right) \times \left\{ \left(\frac{2m - b(R_0)}{2m_s(R_0)}\right)' \right\}^2$$

Now using the expression of  $\left(\frac{m_s}{2R_0}\right)''$  in equation (40) we get,

$$\eta(R_0) \frac{d\sigma^2}{dR} \Big|_{R=R_0} > \frac{1}{2\pi} \left[ \sigma_0 \Xi(R_0) - \frac{\Omega_0}{2\pi R_0} \right] \quad (41)$$

(for details calculation see Appendix)

which gives,

$$\eta(R_0) > \Theta(R_0) \left(\frac{d\sigma^2}{dR}\right)^{-1} \Big|_{R=R_0} \quad \text{if} \quad \frac{d\sigma^2}{dR} \Big|_{R=R_0} > 0 \quad (42)$$

and

$$\eta(R_0) < \Theta(R_0) \left(\frac{d\sigma^2}{dR}\right)^{-1} \Big|_{R=R_0} \quad \text{if} \quad \frac{d\sigma^2}{dR} \Big|_{R=R_0} < 0 \quad (43)$$

$$\text{where } \Theta(R_0) = \frac{1}{2\pi} \left[ \sigma(R_0) \Xi(R_0) - \frac{\Omega_0}{2\pi R_0} \right]$$

For wormhole in four dimensional spacetime, we have  $\frac{d\sigma_0^2}{dR_0} < 0$  (see fig.18). Therefore, we conclude that

$V''(R_0) > 0$ .

Now from the relation  $V'(R_0) = 0$  we get,

the stability of the wormhole is given by equation (43). Next we are interested to search the region where our 4D wormhole model is stable. To obtain the region we have plotted the graph of  $\eta(R_0) = \Theta(R_0) \left(\frac{d\sigma^2}{dR}\right)^{-1} \Big|_{R=R_0}$  which has been shown in Fig. 19. Since the stability region is given by the inequality  $\eta(R_0) < \Theta(R_0) \left(\frac{d\sigma^2}{dR}\right)^{-1} \Big|_{R=R_0}$ . So the region of stability below the graph. Another very interesting thing follows from the plot that  $0 < \eta \leq 1$ . Which is another criterion for stability of the system.

## V. DISCUSSION AND CONCLUDING REMARKS

In the present paper, we have obtained a new class of wormhole solutions in the context of noncommutative geometry background. In this paper we have chosen Lorentzian distribution function as the density function of the wormhole in noncommutative inspired spacetime. We have examined whether wormholes with Lorentzian distribution exist in different dimensional spacetimes. From the above investigations, we see that the wormholes exist only in four and five dimensional spacetimes. In case of five dimension, we have observed that wormhole exists in a very restricted region. From six dimension and onwards the shape function of the wormhole becomes monotonic decreasing due to the presence of the term  $\frac{1}{r^{n-2}}$  in the shape function. So from the above discussion, we can conclude that no wormhole solution exists beyond five dimensional spacetime. In case of four and five dimensional wormholes  $\rho + p_r < 0$  i.e. the null energy conditions are violated. We note that four dimensional wormhole is large enough, however, one can get five dimensional wormhole geometry only in a very restricted region. We have match our interior wormhole solution to the exterior schwarzschild spacetime in presence of thin shell. The linearized stability analysis under small radial perturbation has also been discussed for four dimensional wormhole. We have provided the region where the wormhole is stable and with the help of graphical representation we have proved that the square of the velocity of sound  $0 < \eta \leq 1$

## VI. ACKNOWLEDGEMENT

FR is thankful to the Inter University Center for Astronomy and Astrophysics (IUCAA), India, for providing research facilities.

### Appendix:1

$$m_s = 4\pi R^2 \sigma$$

using the expression of  $\sigma$  we get,

$$\text{or } \frac{m_s}{4\pi R^2} = \frac{1}{4\pi R} \left[ \sqrt{1 - \frac{b(R)}{R} + \dot{R}^2} - \sqrt{1 - \frac{2m}{R} + \dot{R}^2} \right]$$

$$\text{or, } \frac{m_s}{R} = \sqrt{1 - \frac{b(R)}{R} + \dot{R}^2} - \sqrt{1 - \frac{2m}{R} + \dot{R}^2}$$

$$\text{or } \frac{m_s}{R} - \sqrt{1 - \frac{b(R)}{R} + \dot{R}^2} = -\sqrt{1 - \frac{2m}{R} + \dot{R}^2}$$

Squaring bothside we get,

$$\left(\frac{m_s}{R}\right)^2 - 2\frac{m_s}{R} \sqrt{1 - \frac{b(R)}{R} + \dot{R}^2} = \frac{1}{R}(b - 2m)$$

$$\text{or, } \frac{m_s}{R} \left[ \frac{m_s}{R} - 2\sqrt{1 - \frac{b(R)}{R} + \dot{R}^2} \right] = \frac{1}{R}(b - 2m)$$

$$\text{or, } \frac{m_s}{R} - 2\sqrt{1 - \frac{b}{R} + \dot{R}^2} = \frac{1}{m_s}(b - 2m)$$

$$\text{or, } \frac{m_s}{2R} - \frac{b(R) - 2m}{2m_s} = \sqrt{1 - \frac{b(R)}{R} + \dot{R}^2}$$

again squaring bothside we get,

$$\dot{R}^2 = \left(\frac{m_s}{2R}\right)^2 + \left(\frac{b(R) - 2m}{2m_s}\right)^2 + \frac{b + 2m}{2R} - 1$$

Now  $\dot{R}^2 = -V(R)$  which gives,

$$V(R) = 1 - \frac{b + 2m}{2R} - \left(\frac{m_s}{2R}\right)^2 - \left(\frac{b - 2m}{2m_s}\right)^2$$

$$V(R) = F(R) - \left(\frac{m_s}{2R}\right)^2 - \left(\frac{b - 2m}{2m_s}\right)^2$$

where

$$F(R) = 1 - \frac{b + 2m}{2R}$$

### Appendix:2

$$m_s = 4\pi R^2 \sigma$$

$$\text{or, } \frac{m_s}{2R} = 2\pi R \sigma$$

Differentiating bothside with respect to R we get,

$$\text{or, } \left(\frac{m_s}{2R}\right)' = 2\pi(R\sigma' + \sigma)$$

$$= 2\pi R \left\{ -\frac{2}{R}(\sigma + \mathcal{P}) + \Xi \right\} + 2\pi \sigma$$

$$= -4\pi \mathcal{P} + 2\pi R \Xi - 2\pi \sigma$$

Differentiating bothside with respect to R we get,

$$\left(\frac{m_s}{2R}\right)'' = -4\pi \mathcal{P}' + 2\pi(R\Xi' + \Xi) - 2\pi \sigma'$$

Using the value of  $\sigma'$  we get,

$$\left(\frac{m_s}{2R}\right)'' = -4\pi \mathcal{P}' + 2\pi(R\Xi' + \Xi) - 2\pi \left\{ -\frac{2}{R}(\sigma + \mathcal{P}) + \Xi \right\}$$

$$= \frac{4\pi}{R}(\sigma + \mathcal{P}) + 2\pi R \Xi' - 4\pi \eta \sigma'$$

therefore,

$$\left(\frac{m_s}{2R}\right)'' = \Upsilon - 4\pi \eta \sigma'$$

where,

$$\Upsilon = \frac{4\pi}{R}(\sigma + \mathcal{P}) + 2\pi R \Xi'$$

### Appendix:3

$$\begin{aligned} V''(R) &= F''(R) - 2 \left(\frac{m_s(R)}{2R}\right) \left(\frac{m_s(R)}{2R}\right)'' + 2 \left\{ \left(\frac{m_s(R)}{2R}\right)' \right\}^2 \\ &\quad - 2 \left(\frac{2m - b(R)}{2m_s(R)}\right) \left(\frac{2m - b(R)}{2m_s(R)}\right)'' + 2 \left\{ \left(\frac{2m - b(R)}{2m_s(R)}\right)' \right\}^2 \end{aligned}$$

Now  $V''(R_0) > 0$  gives

$$\Omega_0 > 2\pi R_0 \sigma_0 \left(\frac{m_s}{2R_0}\right)''$$

Where

$$\Omega_0 = \frac{F''(R_0)}{2} - 2 \left\{ \left( \frac{m_s(R_0)}{2R_0} \right)' \right\}^2 - \left( \frac{2m - b(R_0)}{2m_s(R_0)} \right) \times$$

$$\left( \frac{2m - b(R_0)}{2m_s(R_0)} \right)'' - \left\{ \left( \frac{2m - b(R_0)}{2m_s(R_0)} \right)' \right\}^2$$

$$\Omega_0 > 2\pi R_0 \sigma [\Xi(R_0) - 4\pi\eta(R_0)\sigma'_0]$$

$$\Omega_0 > 2\pi R_0 \sigma_0 \Xi(R_0) - 4\pi^2 R_0 \eta(R_0) \frac{d\sigma_0^2}{dR_0}$$

$$\frac{\Omega_0}{2\pi R_0} > \sigma(R_0)\Xi(R_0) - 2\pi\eta(R_0)\frac{d\sigma_0^2}{dR_0}$$

$$2\pi\eta(R_0)\frac{d\sigma_0^2}{dR_0} > \sigma_0\Xi(R_0) - \frac{\Omega_0}{2\pi R_0}$$

which gives,

$$\eta(R_0)\frac{d\sigma_0^2}{dR_0} > \frac{1}{2\pi} \left[ \sigma_0\Xi(R_0) - \frac{\Omega_0}{2\pi R_0} \right]$$

- 
- [1] M.Morris, K.Throne, *Am.J.Phys***56**,39 (1988).  
[2] Lobo.F, *Phys.Rev.D* **71** 084011, (2005).  
[3] Rahaman.F ,Kalam.M , Sarker.M, Gayen.K, *Phys.Lett. B* **633**, 161 (2006).  
[4] F Rahaman et al.*Mod.Phys.Lett A***23**,1199 (2008).  
[5] E.Witten,*Nucl.Phys.B* **460** (1996)335; N.Seiberg,E.Witten,*JHEP* **032** (1999)9909.  
[6] A.Smailagic, E. Spallucci, *J.Phys A* **36**,L467 (2003).  
[7] Kourosh Nozaria and S. Hamid Mehdipoura, *JHEP* **0903**, 061, (2009 ).  
[8] F.Rahaman, P.K.F Kuhfittig, K Chakraborty, A.A.Usmani and S.Ray,*Gen.Relativ.Gravit* **44**,905 (2012).  
[9] P.K.F.Kuhfittig,*Adv.High Energy Phys***2012**,462493 (2012).  
[10] Farook Rahaman,Safiqul Islam,P.K.F Kuhfittig and Saibal Ray *Phys.Rev.D***86**,106010 (2012).  
[11] R. Banerjee, B. R. Majhi and S. K. Modak, *Class. Quantum Grav.* **26**, 085010 (2009).  
[12] Farook Rahaman,Ayan Banerjee,Mubasher Jamil, Anil Kumar Yadav,and Humaira Idris, **arXiv:1312.7684[gr-qc]**.  
[13] F. Rahaman, P. K. F. Kuhfittig, B. C. Bhui, M. Rahaman, S. Ray and U. F. Mondal, *Phys. Rev. D* **87**, 084014 (2013).  
[14] Farook Rahaman, Subenoy Chakraborty, Saibal Ray, A. A. Usmani and Safiqul Islam, **arXiv:1209.6291[gr-qc]**.  
[15] F.Rahaman, Saibal Ray, M.Kalam,M.Sarker , *Int J Theor Phys* **48**,3124 (2009).  
[16] Liu.H,Overduin.J.M **Astrophys.J** **538**,386 (2000).  
[17] W. Israel, *Nuovo Cimento B* 44 (1966) 1.  
[18] W. Israel, *Nuovo Cimento B* 48 (1967) 463 (Erratum).